DETC2025-168312

A MULTIDISCIPLINARY DESIGN OPTIMIZATION FRAMEWORK FOR WAVE-DRIVEN DESALINATION SYSTEMS

Nate DeGoede[1]*, **Maha Haji**[1]
[1]Sibley School of Mechanical and Aerospace Engineering
Cornell University
Ithaca, New York 14853
Email: {njd76, maha}@cornell.edu

ABSTRACT

Seawater reverse osmosis (SWRO) desalination offers a critical solution to global water scarcity, but its high energy demand necessitates sustainable power sources. Wave energy converters (WECs) present a promising alternative, particularly wave-driven desalination systems, where they directly pressurize seawater without the inefficiencies of converting to electricity as a middle step. Despite this potential, high costs remain a barrier to widespread adoption.

This study introduces a multidisciplinary design optimization (MDO) framework to enhance wave-driven desalination performance and cost-effectiveness. The framework integrates hydrodynamics, system dynamics, desalination processes, and economic modeling, enabling holistic system-level optimization. A genetic algorithm (GA) is used to find the optimal design, a 58% improvement over a nominal design reported in literature.

Results highlight the importance of balancing WEC, power take-off (PTO), and desalination plant sizing and dynamics. Notably, traditional designs favoring large accumulators and small SWRO plants may benefit from smaller accumulators and increased SWRO plant capacity, reducing the levelized cost of water (LCOW).

This study provides a foundation for cost-effective wave-driven desalination system development, demonstrating the potential of MDO methodologies to improve desalination affordability and sustainability.

———————

*Corresponding Author

1 INTRODUCTION

The world is facing a growing water crisis, with global freshwater demand projected to grow over 40% by 2050 [1]. This rising demand, compounded by factors such as droughts, urbanization, and uneven distribution of water resources, will put immense stress on existing freshwater supplies. Seawater reverse osmosis (SWRO) is a promising solution to mitigate this stress by providing desalinated water. However, SWRO is energy-intensive, requiring 2-4 kWh/m^3 [2]. If powered by fossil fuels, this process would further contribute to climate change, exacerbating water scarcity issues [3]. Therefore, to ensure sustainability, SWRO must be powered by renewable energy sources.

Wave energy converters (WECs) offer a compelling solution. Both SWRO and WECs are marine-based technologies, with SWRO plants typically located on the coast and WECs deployed offshore. Beyond this natural co-location, WECs are particularly suited for SWRO [4] due to their ability to directly pressurize seawater using a hydraulic style power take-off (PTO) system, forming a wave-driven desalination system [5]. Unlike other renewable energy sources that require intermediate energy conversion steps, WECs can provide direct mechanical power, improving overall efficiency.

Despite their potential, WECs face significant economic and technical challenges, with high costs being a primary barrier to widespread adoption. Design optimization is therefore essential for reducing costs and improving performance. Multidisciplinary Design Optimization (MDO) provides a systematic framework for addressing these challenges by integrating

1

multiple interdependent subsystems into a unified design process, allowing for global optimization rather than isolated improvements [6]. MDO-style approaches integrating PTO design with hydrodynamics and/or controls have successfully enhanced electricity-generating WECs, demonstrating its potential to enhance efficiency and energy output [7, 8, 9, 10]. For instance, Michelén Ströfer et al. (2023) achieved a 22% increase in electrical power output using control co-design (CCD) [7], while Grasberger et al. (2024) demonstrated a 60% improvement in normalized power output compared to traditional sequential design methods [10]. These studies emphasize the importance of holistic modeling, which accounts for wave dynamics, WEC operation, PTO performance, and control strategies. Although these studies have shown great promise for MDO to improve WECs, these approaches have yet to be applied to wave-driven desalination systems, leaving a critical gap in research.

This study addresses this gap by developing a holistic MDO framework for wave-driven desalination. A simplified wave-driven desalination system architecture is introduced (Fig 1), where an oscillating surge wave energy converter (OSWEC) drives a piston pump, pressurizing seawater and delivering it to an onshore SWRO plant. The high-pressure seawater enables freshwater production without requiring external energy input. While similar systems have been studied [11, 12, 13, 14], this study excludes an energy recovery unit (ERU)—a component known to enhance efficiency—to focus on the MDO aspects of the system. A comparison between configurations with and without the ERU will be the topic of future work.

The concept sketch in Fig 1 provides an overview of the wave-driven desalination system but does not depict all hydraulic components included in this study. Key elements such as the hydraulic accumulator, pressure relief valve, brine side throttle valve, and directional control valves are omitted for simplicity. A detailed hydraulic circuit diagram, including these components, is shown in Fig 2.

The following sections present the MDO problem formulation, defining the design variables that shape the design space.
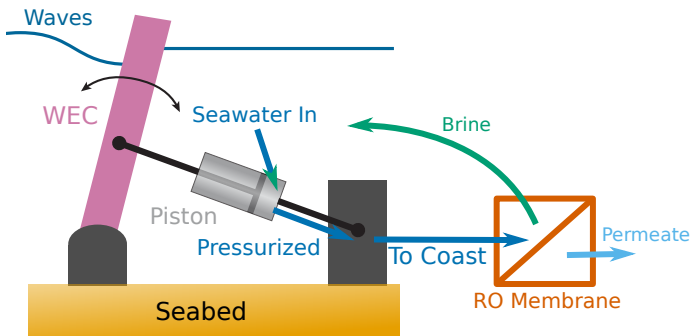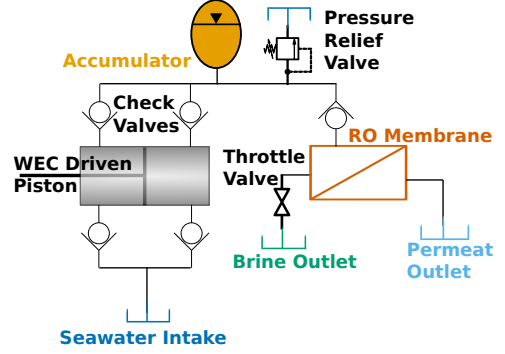

FIGURE 2: HYDRAULIC CIRCUIT DIAGRAM OF THE WAVE-DRIVEN DESALINATION SYSTEM.

A comprehensive wave-driven desalination model is then introduced, structured into key modules: desalination plant, hydrodynamics, system dynamics, and economic analysis. Then a latin hypercube sampling is performed to determine system sensitivity and design variable importance. Finally, the results of the optimization are presented and discussed, highlighting the impact of MDO on the design of wave-driven desalination systems.

2 PROBLEM FORMULATION
2.1 MULTIDISCIPLINARY DESIGN OPTIMIZATION FRAMEWORK

The optimization problem in this study is formally defined as:

$$
\begin{aligned}
\text{Minimize} \quad & \text{LCOW}(\mathbf{x}, \mathbf{p}; \hat{u}) \\
\text{by varying} \quad & \mathbf{x} \\
\text{subject to} \quad & \mathbf{g} \leq 0 \\
& \mathbf{h} = 0 \\
\text{while solving} \quad & \mathbf{R}(\mathbf{x}, \mathbf{p}; \hat{u}) = 0 \\
\text{for} \quad & \hat{u}
\end{aligned}
$$

LCOW (levelized cost of water) is the objective function to be minimized (further discussed in Section 3.4). $\mathbf{x}$ represents a vector of design variables including variables related to WEC geometry, PTO, and the SWRO plant (shown in Table 1). $\mathbf{p}$ represents a vector of parameters related to the design as well as environmental conditions (shown in Appendix A). $\hat{u}$ is the vector of coupled variables. The constraints include inequality constraints ($\mathbf{g} \leq 0$) and equality constraints ($\mathbf{h} = 0$) which are enforced in the system dynamics module, Section 3.3. $\mathbf{R}$ represents the governing equations for different disciplinary modules: seawater desalination, hydrodynamics, system dynamics, and economics.
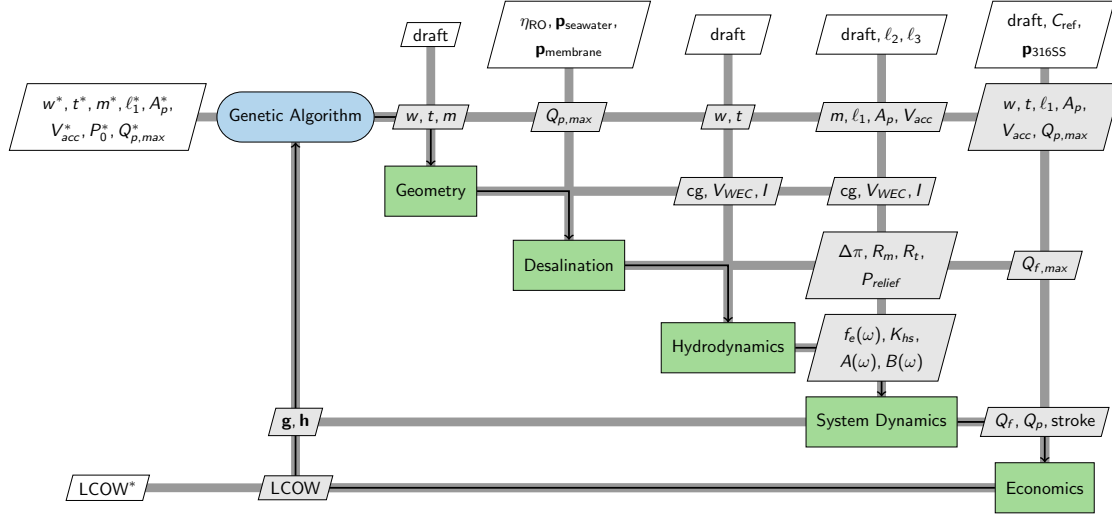

FIGURE 1: SIMPLE WAVE-DRIVEN DESALINATION SYSTEM CONCEPT SKETCH.

FIGURE 3: XDSM DIAGRAM OF THE WAVE-DRIVEN DESALINATION SYSTEM OPTIMIZATION PROBLEM. NOTE $\mathbf{p}_{\text{seawater}}$, $\mathbf{p}_{\text{membrane}}$, AND $\mathbf{p}_{\text{316SS}}$ REPRESENT VECTORS OF PARAMETERS RELATED TO THE MEMBRANE, SEAWATER, AND 316 STAINLESS STEEL, RESPECTIVELY.

These modules are further discussed in the Section 3, System Modeling. Controls are not included at this time, but will be included in future work.

This optimization problem is shown graphically in the xDSM diagram [15] in Fig. 3. The xDSM diagram illustrates module interactions, including their connection with the optimizer (genetic algorithm), LCOW calculation in "Economics," and constraint evaluation ($\mathbf{g}, \mathbf{h}$) in "System Dynamics." Gray lines depict information flow between modules, with gray parallelograms indicating module inputs and outputs, and white parallelograms for optimizer inputs and outputs. Arrows show the sequence of module evaluations.

2.2 DESIGN SPACE

The design vector, $\mathbf{x}$, consists of the following variables: WEC width, w [m], WEC thickness, t [m], WEC mass, m [kg], the distance from the WEC hinge to the PTO joint, ℓ_1 [m], piston area, A_p [m^2], accumulator volume, V_{acc} [m^3], accumulator pre-charge pressure, P_0 [MPa], and SWRO plant capacity, $Q_{p,max}$ [m^3/day]. Table 1 summarizes the design variables, their bounds and nominal values. Some of the key WEC dimensions are shown in Fig. 4 (a).

One notable aspect of the bounds is that the upper bound of ℓ_1 is set to the draft parameter rather than a fixed value. The draft represents the distance from the still water line to the bottom of the WEC float. The WEC width refers to the sway dimension, while the WEC thickness corresponds to the surge dimension. To reduce the dimensionality of the design space, draft and height are excluded as design variables, as the chosen variables already

TABLE 1: DESIGN VARIABLES

Variable	Nominal Value	Lower Bound	Upper Bound
w	18 m	10 m	30 m
t	2 m	1 m	5 m
m	127×10^3 kg	50×10^3 kg	500×10^3 kg
ℓ_1	2 m	0.1 m	draft
A_p	0.26 m^2	0.01 m^2	1 m^2
V_{acc}	4 m^3	0.01 m^3	6 m^3
P_0	3 MPa	1 MPa	7 MPa
$Q_{p,max}$	3150 m^3/day	1000 m^3/day	10000 m^3/day

provide sufficient control over device hydrodynamics. The WEC dimensions are illustrated in Fig. 4 (a). Additionally, to aid in the interpretation of ℓ_1, a mechanism diagram is provided in Fig. 4 (b), which also shows the intake's location defined by ℓ_2 and ℓ_3 (both of which are parameters rather than design variables).

2.3 PARAMETERS AND CONSTRAINTS

The parameters used in this study are similar to those used by Yu and Jenne (2018) [11]. The subcategories of parameters include: general (parameters like gravity and wave conditions), desalination, WEC, mechanism, and solver parameters for the
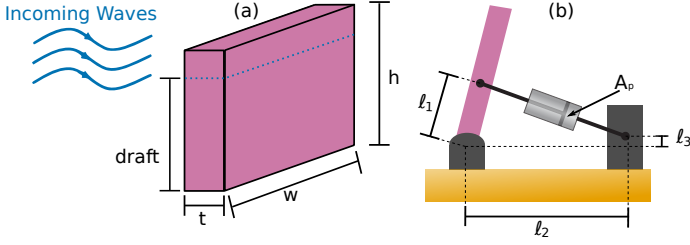
FIGURE 4: WEC (a) AND MECHANISM (b) DIMENSIONS. NOTE THAT h REPRESENTS THE WEC HEIGHT, WHICH IS A PARAMETER RATHER THAN A DESIGN VARIABLE.

different submodules. Full tables of parameters can be found in Appendix A.

Constraints are largely enforced by the system dynamics module (Section 3.3). These constraints are applied to constrain piston motion, ensure the SWRO plant is not operated above capacity, and to ensure force and energy balance within the system.

2.4 OPTIMIZATION ALGORITHM

A genetic algorithm (GA) is the most suitable choice for this problem due to the absence of accessible gradients in the hydrodynamics (Section 3.2) and system dynamics (Section 3.3) modules. While finite differencing these modules is theoretically possible, these modules are highly computationally expensive, making such an approach impractical. Consequently, a heuristic algorithm like a GA is the best choice. A table of the GA hyperparameters is provided in Appendix A Table 3.

3 SYSTEM MODELING

The model shown in Fig. 3 consists of four primary modules: "Desalination", which calculates dependent variables related to the single-stage SWRO plant, "Hydrodynamics", which calculates dependent variables related to the wave-structure interaction, "System Dynamics" which solves the system dynamics of the wave-driven desalination system, and "Economics" which evaluates the LCOW objective. Additionally, a "Geometry" module is included to map variables and parameters to dependent variables across different modules. However, since it does not contribute to independent disciplinary calculations, it is not considered a separate discipline. The four main modules are discussed in more detail in the following subsections.

3.1 DESALINATION MODULE

The desalination module calculates key parameters for the single-stage RO plant, considering the system capacity and seawater composition. The reverse osmosis (RO) process is governed by

$$Q_p = A_w A_m (\Delta P - \Delta \pi), \tag{1}$$

where Q_p [m^3/s] is the permeate flow rate, A_w [m^3/N-s] is the water permeability coefficient, A_m [m^2] is the membrane area, ΔP [Pa] is the pressure difference across the membrane, and $\Delta \pi$ [Pa] is the osmotic pressure difference across the membrane. The osmotic pressure is calculated using [16]:

$$\pi = iCRT, \tag{2}$$

where i [-] is the number of ions produced per molecule of solute, C [mol/m^3] is the concentration of the solute, R [J/K-mol] is the ideal gas constant, and T [K] is the temperature. In this study, we set $\Delta \pi$ to the osmotic pressure of the seawater minus the target permeate osmotic pressure.

For the water permeability coefficient (A_w) we adopt the constant value of 2.57×10^{-12} m^3/N-s, as reported by Yu and Jenne (2018) [11]. This choice is justified by our use of the same SWRO membrane, the SW30HR-380 Dry from DuPont [17], for which their coefficient was determined. The membrane area A_m is then given by

$$A_m = \frac{Q_{p,max}}{Q_0} A_0, \tag{3}$$

where Q_0 and A_0 are the nominal flow rate and membrane area for the SW30HR-380 membrane, found on the datasheet [17].

At this stage, Eq. 1 relates only pressure and flow rate. To integrate this relationship into system dynamics, we define the membrane resistance (R_m [MPa-s/m^3]) as

$$\frac{1}{A_w A_m} \tag{4}$$

This allows for a linearized resistance model, simplifying system-level calculations.

To avoid running the system above capacity, a pressure relief valve is included, with its set pressure P_{relief} [MPa] defined as

$$P_{\text{relief}} = Q_{p,max} R_m + \Delta \pi \tag{5}$$

This equation ensures that if the flow exceeds the system's capacity, the pressure relief valve will open. Notably, by combining Eqs. 3 4 and 5, the dependency on $Q_{p,max}$ cancels out, making P_{relief} independent of specific design parameters under the current membrane resistance model. However, this remains a dependent variable, allowing for flexibility in alternative design spaces or resistance models.

For flow to pass through the membrane, resistance on the brine side is required. This can be achieved using a throttle valve or an ERU (for higher efficiency in advanced designs). In this study we implement a constant throttle valve resistance (R_t [MPa-s/m^3]), calculated such that when the system runs at full capacity, it also runs at the recommended recovery ratio,

4

η_{RO}, given the SW30HR-380 membrane and the specified seawater composition. This recovery ratio was determined using WAVE [18].

$$R_t = \frac{P_{\text{relief}}}{Q_{p,max}(\frac{1}{\eta_{RO}} - 1)} \qquad (6)$$

3.2 HYDRODYNAMICS

Falnes and Kurniawan (2022) [19] define the equation of motion for an oscillating WEC as:

$$I\ddot{\xi} = f_e - f_r - f_b - f_v - f_f - f_u \qquad (7)$$

where I [m or kg-m^2] is the inertia of the WEC, dependent on WEC mass m (a design variable), ξ [m or rad] is the body linear or angular motion, f_e [N or Nm] is the excitation force or torque due to incident waves, f_r [N or Nm] is the radiation force or torque due to the WEC's oscillations, accounting for added mass and radiation damping, f_b [N or Nm] is the hydrostatic force or torque due to buoyancy and restoring effects, f_v [N or Nm] is the drag force or torque which arises from nonlinear viscous effects (neglected in this study), f_f [N or Nm] is the force or torque that captures friction forces (also neglected), and f_u [N or Nm] is the PTO force or torque, which represents energy extraction by the WEC's power conversion system. The PTO force is modeled in the system dynamics module, while drag and friction are omitted, assuming linear potential flow theory. Grasberger et al. (2024) [10] also apply these simplifications in their OSWEC study.

The hydrostatic force, which accounts for the buoyancy of the WEC and its tendency to return to equilibrium, is given by:

$$f_b = K_{hs}\xi, \qquad (8)$$

where K_{hs} is the hydrostatic stiffness matrix.

The radiation force, which accounts for the radiated waves generated by the WEC motion, is expressed as:

$$f_r = A(\omega)\ddot{\xi} + B(\omega)\dot{\xi}, \qquad (9)$$

where $A(\omega)$ and $B(\omega)$ are the added mass and radiation damping matrices, respectively.

This formulation simplifies the WEC hydrodynamics to four key components: the excitation force, hydrostatic stiffness matrix, added mass matrix, and radiation damping matrix. These coefficients are computed using the open-source Boundary Element Method (BEM) solver Capytaine [20]. BEM solvers are well suited for wave-structure interaction problems as they only require meshing of the structure-fluid boundary, unlike computational fluid dynamics solvers which require full fluid volume meshing, significantly reducing computational cost [21].

For this study, the WEC flap is approximated as a rectangular prism, restricted to pitch motion about its bottom hinge. Notably, added mass, radiation damping, and excitation force are all frequency-dependent.

3.3 SYSTEM DYNAMICS

The wave-driven desalination system dynamics are modeled in MATLAB+Simulink, capturing the interactions between the WEC and PTO system. The following sections detail the modeling of each subsystem.

3.3.1 Wave Energy Converter
The WEC dynamics are modeled using WEC-Sim [22], an open-source software developed by the National Renewable Energy Laboratory (NREL) and Sandia National Laboratories. Using hydrodynamic coefficients obtained from the hydrodynamics module, WEC-Sim simulates WEC system dynamics within a Simulink-based framework, enabling efficient analysis of wave-structure interactions and PTO performance. WEC-Sim offers significant advantages over other WEC simulation tools by operating in the time domain, allowing it to capture complex dynamics and nonlinearities that many alternative methods can only approximate. The WEC is modeled as a two body system, with the base fixed to the seafloor and the flap limited to a one degree of freedom (pitch). The WEC model also includes the mechanism to drive the piston. With the intake location, hinge location, and PTO joint location all defined according to Fig. 4.

3.3.2 Power Take-Off
The desalination hydraulic circuit (Fig. 2) is modeled using the isothermal liquid domain from the Simscape Fluids Toolbox. This domain is specialized for modeling hydraulic systems and is a good fit for modeling the dynamics of the hydraulic circuit presented. The high level Simscape PTO model is shown in Fig. 5.

From this high level view, we can see the main components of the hydraulic circuit. The "Piston Cylinder" block contains the piston and directional valves, followed by the accumulator and pressure relief valve, as well as the RO membrane, modeled in the "RO Subsystem" block, and finally the throttle valve on the brine side.

The "Piston Cylinder," modeled after Yu and Jenne's [11], uses a single double-acting piston, though the system dynamics would remain largely unchanged if the piston area variable was distributed across multiple smaller pistons instead of a single large one. It also uses three-way controlled directional valves instead of check valves to simplify computations for the solver while maintaining the overall system dynamics.

The "RO Subsystem" is broken down in Fig. 6. This subsystem includes a check valve to prevent forward osmosis in low energy waves, followed by the membrane resistance and osmotic pressure blocks which allow for a Simscape representation of eq 1. The membrane resistance block is a linear resistance on the
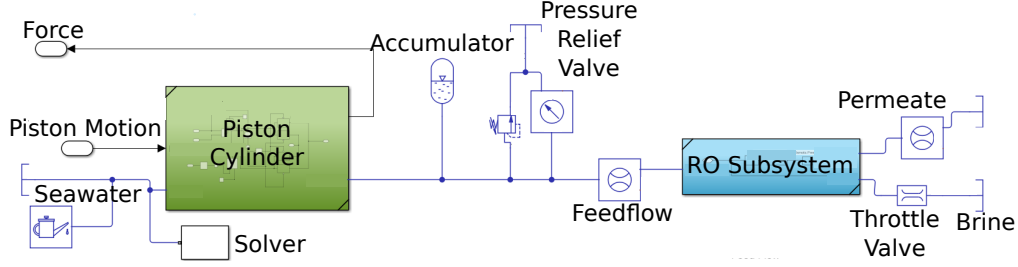
FIGURE 5: SIMSCAPE MODEL OF THE HYDRAULIC CIRCUIT.

volumetric flow rate, and the osmotic pressure block applies a pressure on the permeate side equal to the osmotic pressure difference as calculated in Equation 2.
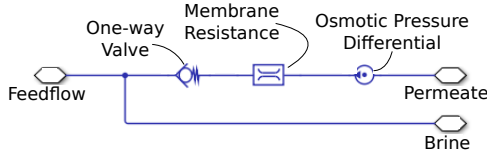

FIGURE 6: SIMSCAPE MODEL OF THE RO MEMBRANE.

3.3.3 Coupled Solver The PTO model (Fig. 5) calculates the force on the piston given the WEC motion solved by WEC-Sim. This force (f_u) is then fed back to WEC-Sim to couple the WEC and PTO dynamics, completing Equation 7. MATLAB's ode4 solver, a fourth order Runge-Kutta solver, with a 0.1 s time step is used to solve the system dynamics.

3.4 ECONOMICS

Our objective is to minimize the levelized cost of water (LCOW) [\$/m^3] which is calculated using the annual water production (AWP) [m^3/year] from the system dynamics module and the costs calculated from the economic module. We consider a simple cost model comprised of two categories: capital (CAPEX) and operational expenditures (OPEX). The LCOW is then determined by

$$\text{LCOW} = \frac{(\text{FCR} \times \text{CAPEX}) + \text{OPEX}}{\text{AWP}}, \qquad (10)$$

where FCR is the fixed charge rate, 10.8% based on the assumptions made in the U.S. Department of Energy report [23]. We note that Eq. 10 takes a form similar to that of the levelized cost of energy (LCOE) used by the U.S. Department of Energy [23]. The CAPEX and OPEX are split into three sections based on the three main sections of design variables: the WEC, the PTO, and the desalination plant. It is important to note that this cost model is not meant to provide an exact representation of total system costs. Instead it serves as a tool to quantify relative cost savings

between different designs, highlighting the impact of applying an MDO approach to this problem. An explanation of the cost model for each component is given below. Note that all costs are adjusted to 2025 USD.

3.4.1 Wave Energy Converter Cost modeling for WECs is inherently uncertain due to limited real world data, making it difficult to achieve high accuracy. This presents a significant challenge for studies like this, where levelized cost is used as an objective function. Despite these challenges, a practical and comparative cost model can still be developed to capture key cost trends and enable design comparisons. In this study, we follow the method from Grasberger et al. (2024) who introduced a simplified cost model for their OSWEC CCD study [10]. In this model, costs are expressed as a function of the float's surface area of the float through a combination of linear and logarithmic terms, shown below

$$\text{Cost} = C_{1,ref}\left(\frac{A_x}{A_{ref}}\right) + C_{2,ref}\left(1 + \log\left(\frac{A_x}{A_{ref}}\right)\right), \qquad (11)$$

where A_x [m^2] is the surface area of the float, A_{ref} [m^2] is the surface area of the reference float, and $C_{1,ref}$ [\$] and $C_{2,ref}$ [\$] are the costs of the reference float associated with the two terms. The linear term captures cost associated with the structural components (the flap, base, and mooring), while the logarithmic term captures other expenses (PTO, monitoring, other OPEX) which are less dependent on the size of the float. This cost model relies on an accurate reference WEC for meaningful comparisons.

Given the importance of a reliable reference WEC, we utilize NREL's Reference Model 5 (RM5) [24], a well-documented OSWEC. Its similarity to the WEC design in this study makes it an appropriate benchmark for cost comparison and performance evaluation. To tailor the cost model to this study's specific WEC design, we exclude certain cost components that are not relevant or do not scale directly with WEC size. In particular, since this design replaces an electricity-generating PTO with the SWRO PTO, the electrical PTO costs from the initial RM5 cost model are not included. Instead, we determine SWRO PTO specific costs, detailed in the next section. Additionally, because this

study considers a nearshore fixed-bottom WEC, many mooring-related expenses from RM5 are not included. Finally, many transit and other overhead design costs are excluded as they are unlikely to scale proportionally with the size of the WEC.

3.4.2 Power Take-Off

The PTO cost model covers the costs associated with the accumulator and the piston cylinder. The accumulator cost is modeled as function of the accumulator volume (V_{acc})

$$\text{Cost} = 1.621 \times 10^5 V_{acc}^{0.986}, \tag{12}$$

where the two constants are tuned to approximate quotes from a supplier [25].

The piston cylinder cost is modeled as a function of the required volume of steel (V_{316}).

$$\text{Cost} = C_{316}\rho_{316}V_{316}(1+L), \tag{13}$$

where C_{316} [$/lb] is the unit cost of 316 stainless steel, ρ_{316} [lb/in^3] is the density of 316 stainless steel, and L is a cost multiplier to account for labor. The volume of steel is calculated as:

$$V_{316} = V_{\text{cylinder}} + 2V_{cap} + V_{\text{piston}} + V_{textrod}, \tag{14}$$

where V_{cylinder} [in^3] is the volume of the cylinder, V_{piston} [in^3] is the volume of the piston, V_{cap} [in^3] is the volume of the end caps, and V_{rod} [in^3] is the volume of the rod. The thicknesses of the cylinder and end caps are calculated using the ASME Boiler and Pressure Vessel Code [26]. The piston volume uses the same thickness as the end caps. The required rod diameter is calculated to prevent buckling failure and tensile/compressive failure. Required stroke length, which is a factor for the length of the cylinder is determined by the system dynamics solver. The various coefficients used in the piston cylinder cost model can be found in Appendix A Table 7.

3.4.3 Desalination Plant

The costs associated with the desalination plant are divided into two categories: capital costs and operational costs. The capital costs includes all expenses related to the construction and installation of the plant, while the operational costs over the recurring costs associated with its annual operation and maintenance.

Cost models for small- to mid-scale SWRO desalination plants of this scale (producing thousands of m^3/day) are scarce and often poorly documented or inconsistently implemented. Most well-documented economic studies focus on large-scale plants (hundreds of thousands of m^3/day) [27, 28, 29, 30], making them less applicable to this study. Meanwhile, studies that examine smaller desalination plants frequently lack transparent methodologies for estimating SWRO-specific plant costs

[31,32]. One notable study on wave-driven desalination employs the Desalination Economic Evaluation Program (DEEP 5.1) developed by the International Atomic Energy Agency to estimate unit CAPEX cost [33]. However, DEEP 5.1 itself is poorly documented [34], making it difficult to assess the accuracy and reliability of its cost estimates.

Given these limitations, this study adopts a cost estimation methodology based on the work of Voutckov in *Desalination Project Cost Estimating and Management* [35]. Using the cost curves provided in sections 4 (CAPEX) and 5 (OPEX) of his work, a flexible cost model is developed that can be customized for different project specifications. Each curve is fitted to a power function, chosen to prevent unrealistic behavior at the lower end of the scale. Unlike polynomial fits, which can produce unrealistic negative costs, a power-law fit ensures a monotonic and physically meaningful cost relationship.

3.5 VALIDATION

Since one of the contributions of this study is the development of a new modeling framework, it is difficult to validate the entire system against a single reference. Instead, each module is validated separately. The desalination module is built on textbook equations, and the results of the module have been confirmed to return expected results. The hydrodynamics module is built using a trusted open-source BEM solver, Capytaine [20], with irregular frequency removal, and the number of panels is carefully chosen depending on WEC size to ensure convergence of the hydrodynamic coefficients. The system dynamics module was validated against Yu and Jenne (2018) [11] by using the modular components of this paper's model to reproduce the results of their model. The differences (9%) in the results have been confirmed to be attributed to WEC-Sim updates. After validation, the modular components were reassembled into the new simplified PTO design. Additionally, the RO component was replaced with the one in Fig. 6, which the authors believe better represents the RO process.

The economics module was the most difficult to validate, as there is little data on the costs of small- to mid-scale desalination plants. The WEC cost model was validated against the NREL RM5 [24] cost model. The piston and accumulator cost models were validated to capture trends observed in supplier data. The cost model for the desalination plant had each component of the cost validated against selected points on the cost curves in Voutchkov (2018) [35]. Then the full desalination plant cost was validated against the cost estimates from Yu and Jenne (2017) [37]. This study found a much larger CAPEX and a much smaller OPEX, but the cost was of the same order of magnitude and the authors believe this cost model is an improvement upon the previous work.

4 DESIGN OF EXPERIMENTS

A preliminary design of experiments (DOE) study provides valuable insights into the relative importance of design variables and relations between them and performance objectives.

For this study, we use a Latin Hypercube sampling method with 508 samples to explore the design space. To quantify the importance of each design variable, we employ feature importance analysis using a random forests regression model trained on the DOE dataset [36]. We compute feature importance using both mean decrease in impurity and permutation importance. These metrics indicate how much each variable contributes to predicting LCOW, helping identify potential reductions in design space complexity. The feature importance results are shown in Fig. 7. Fig 7 (a) shows the results for the full DOE dataset, while Fig 7 (b) shows the results for a filtered subset of designs with LCOW < 10 \$/m^3. This filtering is used to compare the importance of design variables for creating reasonable designs (a) versus improving already reasonable designs (b).

The DOE results indicate that all design variables significantly impact LCOW prediction, making design space reduction inadvisable. However, P_0 and ℓ_1 appear most important for ensuring reasonable designs. Their importance decreases in the filtered dataset (Fig. 7 (b)), suggesting that while they are the main drivers for feasibility, other variables are of similar importance for improving already reasonable designs.

5 OPTIMIZATION RESULTS

The optimizer successfully converged after 323 generations (Fig. 8). The optimal design minimizing LCOW is presented in Table 2, alongside a nominal design from the literature for comparison [37]. Notably, LCOW of the nominal design is recalculated using the model presented in this study, which differs from the value reported in the original source. Additionally, no optimized variables lie on the design space bounds, indicating the bounds are not overly restrictive.

6 DISCUSSION

The result of the optimization reveal several key takeaways. The first takeaway is the large improvement in LCOW from the nominal design to the optimized design. The optimized design has an LCOW of 1.68 \$/m^3, a 58% reduction from the nominal design's LCOW of 3.97 \$/m^3. This suggests that the MDO framework is effective in improving system performance and reducing costs.

The second takeaway is that the optimized design suggests a departure from conventional design trends in the literature. Specifically, the design features a smaller accumulator volume (4.57 m^3) and a larger desalination capacity (4882 m^3/day). In contrast, previous studies have favored larger accumulators to
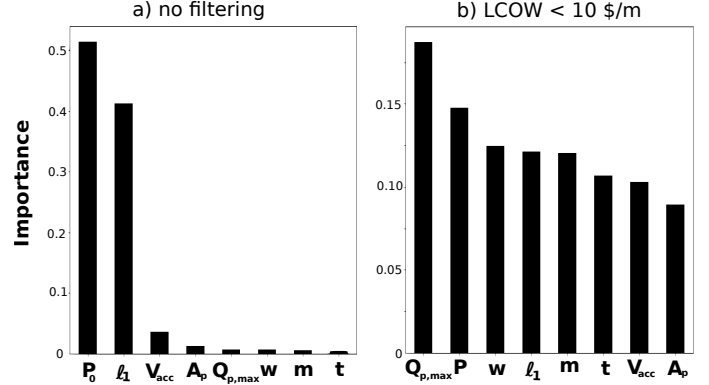
FIGURE 7: FEATURE IMPORTANCE OF DESIGN VARIABLES. THE FULL SAMPLING RESULTS ARE SHOWN IN (a), WHILE A FILTERED SUBSET (284 OF 508) OF RESULTS ARE SHOWN IN (b).
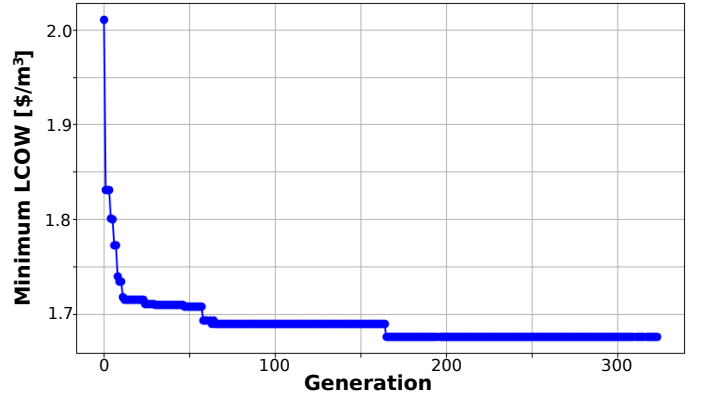
FIGURE 8: GA CONVERGENCE PLOT.

smooth fluctuations in feedwater flow. In their economic assessment of wave-driven desalination, Yu and Jenne used an accumulator volume of 6 m^3 (2017) for a 3100 m^3/day plant [37]. Brodersen et al. (2022) used a 6 m^3 accumulator for a 1700-2400 m^3/day desalination plant [38]. These studies assumed that large accumulators improve feedwater regulation, allowing smaller desalination plants to capture a higher percentage of the flow. While this logic holds when ignoring accumulator costs, the optimization suggests that reducing accumulator volume and increasing desalination plant capacity can lead to a lower LCOW, further reinforcing the need for a holistic model when designing a wave-driven desalination system.

The third takeaway is the vast difference in WEC design and mechanism between the design from literature and the optimized design. The optimized design features a smaller WEC and a smaller effective "gear ratio" (the combination of ℓ_1 and A_p

TABLE 2: OPTIMIZED DESIGN VARIABLES

Variable	MDO Suggestion	Nominal Design [37]
w	11.3 m	18 m
t	1.99 m	1.8 m
m	$396{\times}10^3$ kg	$127{\times}10^3$
ℓ_1	3.25 m	1.9 m
A_p	0.859 m^2	0.26 m^2
V_{acc}	4.57 m^3	6 m^3
P_0	5.95 MPa	3.00 MPa
$Q_{p,max}$	4882 m^3/day	3100 m^3/day
LCOW	1.68 \$/m^3	3.97 m^3/day

which together define the mechanical advantage from WEC motion to feedwater flow). This suggests that the WEC and mechanism design from literature is more suited for high pressure hydraulic systems. This makes sense when we consider that the design from literature [37] is a slightly modified RM5 [24] design, which was designed to reach 28 MPa while SWRO only requires 5 MPa. Although the design from literature is modified slightly to reflect this lower pressure (smaller flap, larger piston area), the optimizer suggests that the design is still not optimal for the lower pressure system. The heavier WEC likely improves impedance matching between the WEC and the wave spectrum. Therefore, an uncertainty analysis would be useful to determine a robust performance metric.

7 CONCLUSION

This study introduces an MDO framework for wave-driven desalination system design. Optimization results demonstrate that the MDO framework effectively reduces the levelized cost of water (LCOW) by 58% compared to a nominal design from literature. The optimized design suggests a departure from conventional design trends, indicating that smaller accumulator sizes and larger desalination plant capacities can lead to lower LCOW. This finding emphasizes the importance of holistic optimization, as inadequate coordination between subsystems may result in inefficiencies and increased costs.

Future work should focus on:

1. Fully developing the PTO cost model by including piston and mechanism costs.
2. Adding control to the system dynamics model, with declutching control [39] identified as a particularly promising approach for wave-driven desalination.

3. Comparing MDO results to those obtained through traditional sequential design optimization.
4. Developing gradient-compatible models for the hydrodynamics and system dynamics modules to enable gradient-based optimization.
5. Investigating different wave-driven desalination PTO architectures, such as incorporating an ERU, within this framework.

The MDO framework presented in this study provides a systematic approach to optimizing wave-driven desalination systems, offering new pathways for improving desalination affordability and sustainability. Future advancements in control strategies, economic modeling, and real-world implementation will further strengthen the feasibility of wave-powered desalination as a scalable solution to global freshwater challenges.

REFERENCES

[1] Eliasson, J., 2015. "The rising pressure of global water shortages". *Nature, 517*(6), Jan.
[2] Li, Z., Siddiqi, A., Anadon, L. D., and Narayanamurti, V., 2018. "Towards sustainability in water-energy nexus: Ocean energy for seawater desalination". *Renewable and Sustainable Energy Reviews, 82*, Feb., pp. 3833–3847.
[3] Gillis, J., 2015. "California drought is made worseby global warming, scientists say". *New York Times*, Aug.
[4] of Energy, U. D., 2019. Powering the blue economy: Exploring opportunities for marine renewable energy in maritime markets, 4.
[5] Davies, P., 2005. "Wave-powered desalination: resource assessment and review of technology". *Desalination, 186*(1–3), Dec., pp. 97–109.
[6] Sobieszczanski-Sobieski, J., 1995. "Multidisciplinary design optimization: An emerging new engineering discipline". *Solid Mechanics and Its Applications*, p. 483–496.
[7] Ströfer, C. A. M., Gaebele, D. T., Coe, R. G., and Bacelli, G., 2023. "Control co-design of power take-off systems for wave energy converters using wecopttool". *IEEE Transactions on Sustainable Energy, 14*(4), Oct., pp. 2157–2167.
[8] Peña-Sanchez, Y., García-Violini, D., and Ringwood, J. V., 2022. "Control co-design of power take-off parameters for wave energy systems". *IFAC-PapersOnLine, 55*(27), pp. 311–316.
[9] Rosati, M., and Ringwood, J. V., 2023. "Control co-design of power take-off and bypass valve for owc-based wave energy conversion systems". *Renewable Energy, 219*, Dec., p. 119523.
[10] Grasberger, J., Yang, L., Bacelli, G., and Zuo, L., 2024. "Control co-design and optimization of oscillating-surge wave energy converter". *Renewable Energy, 225*, May, p. 120234.

[11] Yu, Y.-H., and Jenne, D., 2018. "Numerical modeling and dynamic analysis of a wave-powered reverse-osmosis system". *Journal of Marine Science and Engineering, 6*(4), Nov., p. 132.

[12] Suchithra, R., Das, T. K., Rajagopalan, K., Chaudhuri, A., Ulm, N., Prabu, M., Samad, A., and Cross, P., 2022. "Numerical modelling and design of a small-scale wave-powered desalination system". *Ocean Engineering, 256*, July, p. 111419.

[13] Mi, J., Wu, X., Capper, J., Li, X., Shalaby, A., Wang, R., Lin, S., Hajj, M., and Zuo, L., 2023. "Experimental investigation of a reverse osmosis desalination system directly powered by wave energy". *Applied Energy, 343*, Aug., p. 121194.

[14] Simmons, J., 2024. "Modeling and design of hydraulic power take-offs for ocean wave-powered reverse osmosis desalination". PhD thesis, University of Minnesota, 4.

[15] Lambe, A. B., and Martins, J. R. R. A., 2012. "Extensions to the design structure matrix for the description of multidisciplinary design, analysis, and optimization processes". *Structural and Multidisciplinary Optimization, 46*(2), pp. 273–284.

[16] Seader, J. D., Henley, E. J., and Roper, D. K., 2011. *SEPARATION PROCESS PRINCIPLES: Chemical and Biochemical Operations*, 3rd ed. Wiley.

[17] DuPont, 2024. Filmtec™ sw30hr-380 element product data sheet. Datasheet, Oct.

[18] DuPont. Wave design software.

[19] Falnes, J., and Kurniawan, A., 2020. *Ocean Waves and Oscillating Systems: Linear Interactions Including Wave-Energy Extraction*, 2nd ed. Cambridge University Press.

[20] Ancellin, M., and Dias, F., 2019. "Capytaine: a Python-based linear potential flow solver". *Journal of Open Source Software, 4*(36), apr, p. 1341.

[21] Newman, J., and Lee, C.-H., 2002. "Boundary-element methods in offshore structure analysis". *Journal of Offshore Mechanics and Arctic Engineering, 124*, 05, p. 81.

[22] Wec-sim (wave energy converter simulator).

[23] LaBonte, A., O'Connor, P., Fitzpatrick, C., Hallett, K., and Li, Y., 2013. "Standardized cost and performance reporting for marineand hydrokinetic technologies". In 1st Marine Energy Technology Symposiumt.

[24] Y.-H. Yu, D. J., R. Thresher, A. Copping, S. G., and Hanna, L., 2015. Reference model 5 (rm5): Oscillating surge wave energy converter. Tech. Rep. Report, Jan.

[25] ReasonTek, 2025. Low pressure accuumulator quote, 03.

[26] American Society of Mechanical Engineers, 2015. *Boiler and Pressure Vessel Code, Section VIII, Division 1: Rules for Construction of Pressure Vessels*. ASME, New York. ASME BPVC-VIII-1-2015.

[27] Slocum, A. H., Haji, M. N., Trimble, A. Z., Ferrara, M., and Ghaemsaidi, S. J., 2016. "Integrated pumped hydro reverse osmosis systems". *Sustainable Energy Technologies and Assessments, 18*, Dec., pp. 80–99.

[28] Haefner, M. W., and Haji, M. N., 2023. "Integrated pumped hydro reverse osmosis system optimization featuring surrogate model development in reverse osmosis modeling". *Applied Energy, 352*, Dec., p. 121812.

[29] Huehmer, R., Gomez, J., Curl, J. M., and Moore, K., 2011. "Cost modeling of desalination systems". In International Desalination Association World Congress, International Desalination Association World Congress, International Desalination Association World Congress.

[30] Wittholz, M. K., O'Neill, B. K., Colby, C. B., and Lewis, D., 2008. "Estimating the cost of desalination plants using a cost database". *Desalination, 229*(1–3), Sept., pp. 10–20.

[31] Elkadeem, M. R., Kotb, K. M., Sharshir, S. W., Hamada, M. A., Kabeel, A. E., Gabr, I. K., Hassan, M. A., Worku, M. Y., Abido, M. A., Ullah, Z., Hasanien, H. M., and Selim, F. F., 2024. "Optimize and analyze a large-scale grid-tied solar pv-powered swro system for sustainable water-energy nexus". *Desalination, 579*, June, p. 117440.

[32] Gökçek, M., and Gökçek, O. B., 2016. "Technical and economic evaluation of freshwater production from a wind-powered small-scale seawater reverse osmosis system (wp-swro)". *Desalination, 381*(site.), Mar., pp. 47–57.

[33] Yu, Y.-H., and Jenne, D., 2017. "Analysis of a wave-powered, reverse-osmosis system and its economic availability in the united states". In International Conference on Ocean, Offshore and Arctic Engineering.

[34] Agency, I. A. E., 2013. "Deep 5 user manual".

[35] Voutchkov, N., 2019. *Desalination project cost estimating and management*. CRC Press.

[36] Rogers, J., and Gunn, S., 2006. "Identifying feature relevance using a random forest". In SLSFS 2005, C. Saunders et al., eds., Vol. 3940 of *LNCS*, Springer, p. 173–184.

[37] Yi-Hsiang Yu, D. J., 2017. "Analysis of a wave-powered, reverse-osmosis system and its economic availability in the united states". In Proceedings of the ASME 2017 36th International Conference on Ocean, Offshore and Arctic Engineering OMAE2017.

[38] Brodersen, K. M., Bywater, E. A., Lanter, A. M., Schennum, H. H., Furia, K. N., Sheth, M. K., Kiefer, N. S., Cafferty, B. K., Rao, A. K., Garcia, J. M., and Warsinger, D. M., 2022. "Direct-drive ocean wave-powered batch reverse osmosis". *Desalination, 523*, Feb., p. 115393.

[39] Ringwood, J. V., Bacelli, G., and Fusco, F., 2014. "Energy-maximizing control of wave-energy converters: The development of control system technology to optimize their operation". *IEEE Control Systems, 34*(5), Oct., pp. 30–55.

[40] Shane, 2025. Comprehensive guide to stainless steel pricing and grades, March. Accessed: 2025-05-14.

A TABLES OF PARAMETERS

TABLE 3: GENETIC ALGORITHM HYPERPARAMETERS

Parameter	Value	Units
population size	256	-
number of generations	300	-
mutation rate	0.02	-
crossover rate	0.8	-
number of elites kept	3	-
tournament size	4	-
bits per variable	8	-

TABLE 4: GENERAL PARAMETERS

Parameter	Value	Units
gravitational acceleration	9.81	m/s^2
ocean density	1025	kg/m^3
distance to shore	500	m
ocean temperature	298.15	K
water depth	12	m
wave direction	0 [11]	degrees
wave spectrum	Pierson–Moskowitz [11]	-
significant wave height	2.64 [11]	m
peak period	9.86 [11]	s
Fixed Charge Rate	10.8 [23]	%

TABLE 5: SWRO PARAMETERS

Parameter	Value	Units
feedflow total dissolved solids	35946 [11]	mg/L
permeate total dissolved solids	150 [11]	mg/L
salt molar weight	58.44	g/mol
water permeability coefficient	2.57×10^{-12} [11]	m^3/N-s
recovery ratio	44.2 [18]	%
single SW30HR-380 area	35 [17]	m^2
single SW30HR-380 flow rate	24.6 [17]	m^3/day

TABLE 6: WEC PARAMETERS

Parameter	Value	Units
draft	9	m
cg draft factor	-0.7778	-
unit inertia	14.57	m^2
RM5 surface area	1214 [24]	m^2
RM5 flap cost	3364648.63 [24]	$
RM5 base cost	1706415.27 [24]	$
RM5 bearings cost	17420.34 [24]	$
RM5 mooring cost	997819.2 [24]	$
RM5 monitoring cost	616480.27 [24]	$/yr
RM5 marine operations cost	101387.23 [24]	$/yr
RM5 shore operations cost	347280.29 [24]	$/yr
RM5 parts cost	86237.2 [24]	$/yr
RM5 consumables cost	17480.19 [24]	$/yr
RM5 insurance rate	2 [24]	%

TABLE 7: PTO PARAMETERS

Parameter	Value	Units
ℓ_2	4.7	m
ℓ_3	0	m
max piston stroke	20	m
SS316 cost	2.00 [40]	$/in^3
SS316 density	0.29 [40]	lb/in^3
SS316 yield strength	206 [40]	MPa
SS316 Young's modulus	164 [40]	GPa
cylinder factor of safety	6	-
rod factor of safety	1.5	-
labor factor	0.7	-
end cap attachment factor	0.3 [26]	-
cylinder joint efficiency	0.8 [26]	-

TABLE 8: SOLVER PARAMETERS

Parameter	Value	Units
BEM frequencies	0.2, 0.34, 0.48, ..., 3	rad/s
SysDyn time step	0.1	s
SysDyn sim time	300	s